Disk Galaxy Rotation Curves and Dark Matter Halos

Thorben Mense

June 3, 2018

Contents

1 Introduction

The kinetics of celestial bodies can tell us a lot about their properties, of which the mass is best determined. In the solar system the motion of larger bodies follows the laws of keplarian motion and thus the same was expected for stars in galaxies. Consequently astronomers around the world were puzzled when the first, reliable observations of galactic rotation curves did not match this model [RF70]. With more precise measurements the results of the first observations were cemented and the theory of non-luminous matter which spreads out far beyond the luminous matter, arose [RFT80]. This non-luminous matter, often called Dark Matter, which is thought to have such a huge impact on the

kinematics of galaxies, remains a mystery, as it has not been observed until today.

2 Early Observations of Galaxy Rotation Curves [RF70, RFT80]

2.1 Rotation of the Andromeda Nebula from a Spectroscopic Survey of Emission Regions, Rubin & Ford 1970

As M31, also known as Andromeda, is the closest spiral galaxy we can observe, it has been studied for quite some time. So when it came to observing the kinematics of galaxies it was natural to first look at the velocities in Andromeda. Measuring these velocities proved to be challenging due to technical limitations. Rubin and Ford thus used a new DTM image tube spectrograph which Kent Ford build in the early 1960s. This allowed for the spectral observation of much fainter objects and reliable velocity measurements of Andromeda.

To observe the velocity distribution in the disk of Andromeda Rubin and Ford picked 67 HII emission regions in Andromeda and calculated the velocities from the shift the Hα, the $[O\,III]$ λ5007 and the $[N\,II]$ λ6583 line. Additionally they observed the velocities for regions closer to the core (R<3.2kpc) using the shift of the $[N\,II]$ λ6583 which was prominent at this radii.

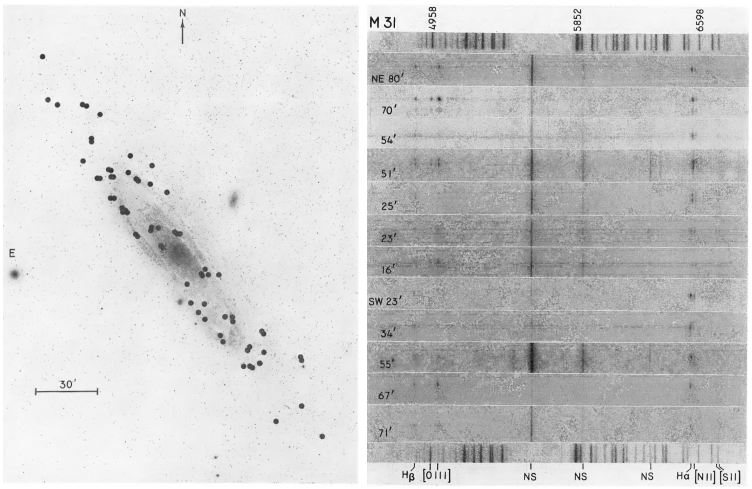

Figure 1: *Left:* UV photograph of Andromeda with the observed HII regions marked with dark dots; *Right:* Representative spectra of emission arranged according to distance from center with a Ne + Fe comparison spectrum on top and bottom.

The observed velocities were corrected for the projection effects and the

total velocity of Andromeda with respect to the Milky Way and were plotted as function of the distance to the galaxies center, the so called velocity curve.

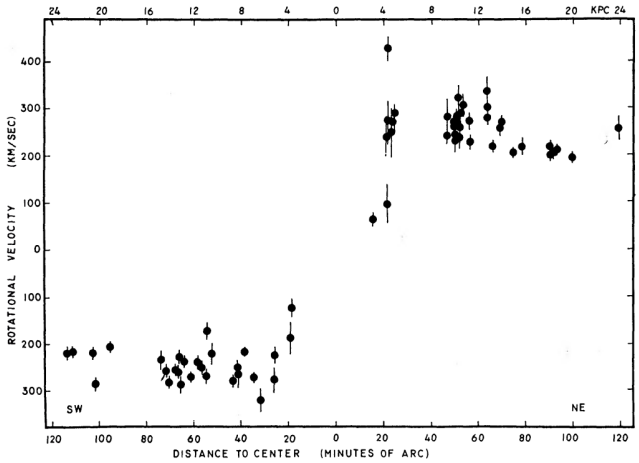

Figure 2: Rotational velocities for sixty-seven emission regions in M31, as a function of distance from the center. Error bars indicate average error of rotational velocities.

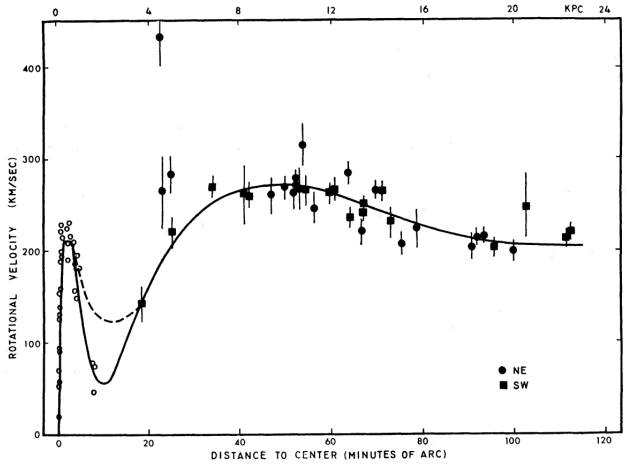

Figure 3: Rotational velocities for OB associations in M31, as a function of distance from the center. For R $<$ 12', curve is fifth-order polynomial; for R $>$ 12', curve is fourth-order polynomial required to remain approximately at near R $>$ 120'. Dashed curve near R = 10' is a second rotation curve with higher inner minimum.

For the observation of Andromeda this rotation curve shows a steep incline

close to the nucleus while the curve is essentially flat for larger radii.

2.2 Rotational properties of 21 SC galaxies with a large range of luminosities and radii, Rubin, Ford & Thonnard 1980

Due to technical improvements spectroscopic data of other galaxies became available so that in 1980. Rubin, Ford & Thonnard were able to observe rotation curves for 21 SC galaxies. For the observations the Kitt Peak 4m RC Spectrograph with a Carnegie image tube was used. The produced spectra were then measured using a Mann two-dimensional measuring engine at the Department of Terrestrial Magnetism, allowing for precise determination of the shifts. From the shift of $H\alpha$ and $[NII]$ $\lambda\lambda$6548, 6583 lines the velocities were calculated using

$$V = c\frac{(\lambda - \lambda_0)}{\lambda_0} \tag{1}$$

with an internal accuracy of $\pm 3km/s$. In the case of unclear identification of the $H\alpha$ or $[NII]$ lines $[SII]$ lines were used additionally.

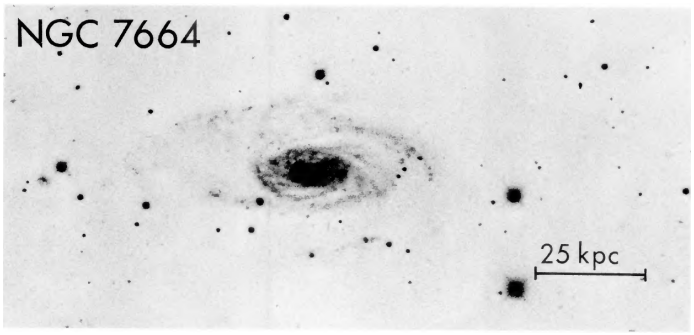

Figure 4: Image of NGC 7664, one of the observed Sc galaxies

To generate a rotation curve from the measured velocities the measurements were projekted to the velocities in the plane of each galaxy using the following formula:

$$V(R) = \frac{(V_{obs} - V_0)\left[\sec^2 i - \tan^2 i \cos^2(\eta - \phi)\right]^{\frac{1}{2}}}{\sin i \cos(\eta - \phi)} \tag{2}$$

$$R = s\left[\sec^2 i - \tan^2 i \cos^2(\eta - \phi)\right]^{\frac{1}{2}} \tag{3}$$

Where s is the nuclear distance on the plane of the sky, R is the nuclear distance in the plane of the Galaxy, ϕ is the angle of the major axis, η is the position angle of the spectrum and i is the inclination of the galaxy. By doing this the rotation curves of the galaxies can be compared and the mean rotational speeds can be described as a funktion of radius.

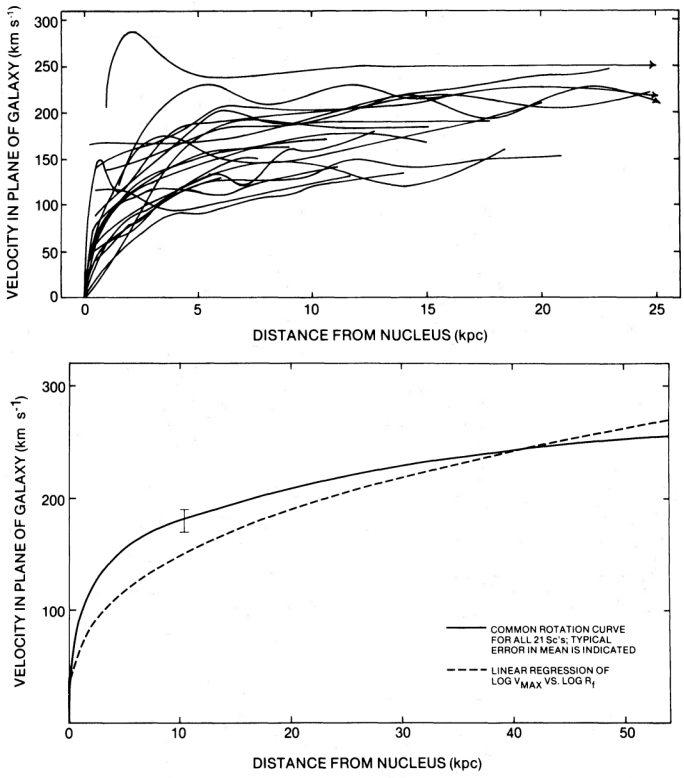

Figure 5: *Top:* Superposition of all 21 Sc rotation curves; *Bottom:* Rotational velocity as a function of radius for all 21 sc galaxies.

The resulting rotation curves (see fig. 5) show behavior similar to the earlier observed Andromeda. In general the rotational velocities increase with the radius, which is not expected if one assumes Keplarian motion. This leads Rubin, Ford and Thonnard to following conclusion:

> "This form for the rotation curves implies that the mass is not centrally condensed, but that significant mass is located at large R. The integral mass is increasing at least as fast as R. The mass is not converging to a limiting mass at the edge of the optical image. The conclusion is inescapable that non luminous matter exists beyond the optical galaxy."

The concept of the mentioned non luminous matter, or dark matter, has since been used to explain the non-Keplarian kinematics of galaxies.

3 Connecting Rotation Curves to the Distribution of Dark Matter in Halos [PSS96, NFW96, NFW97]

3.1 Persic, Salucci & Stel 1996

To further analyze the connection of rotation curves to the properties of galaxies Persic, Saluci and Stel looked at a sample of about 1100 optical and radio rotation curves together with relative surface photometry data. The data was then analyzed statistically to investigate scaling properties between dark and luminous galactic structure parameters.

The set of rotation curves they used consist of 131 reliably sampled rotation curves, while the rest of the samples are synthesized and originate from a paper written in 1995 by Persic and Salucci. The individual rotation curves are normalized to the optical radius, which is the radius encompassing 83% of the total integrated light, and then binned into 11 luminosity and 11 velocity bins and subsequently co-added to form 22 synthetic rotation curves.

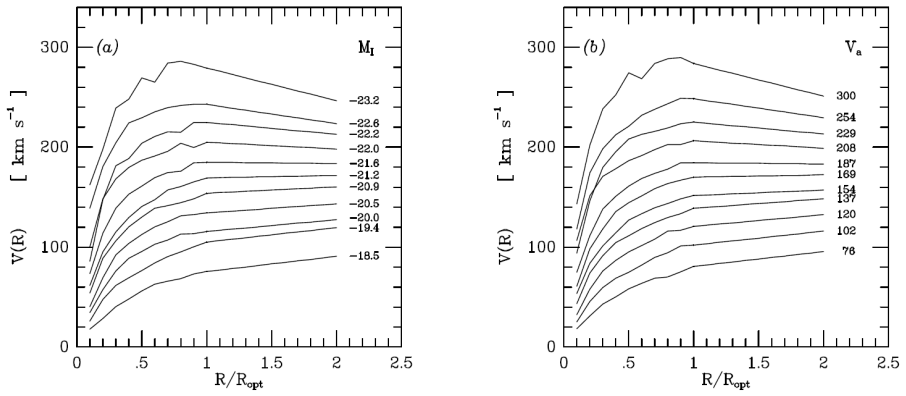

Figure 6: The synthesized rotation curves. *Left:* Binned by luminosity. *Right:* Binned by velocity at R_{opt}

For the further analysis two quantities are introduced: $\nabla - \nabla_{lum}$ and $\delta - \delta_{lum}$.

$\nabla - \nabla_{lum}$ is the discrepancy of the average slope of the rotation curve between 0.6 and 1 R_{opt}, where ∇ is the slope of the actual rotation curve and ∇_{lum} is the slope of a theoretical rotation curve in which the luminous matter traces all the mass.

$\delta - \delta_{lum}$ indicates level the mass discrepancy inside R_{opt}, where $\delta \equiv \left[\frac{V(2R_{opt}) - V(R_{opt})}{V(R_{opt})}\right]$ is the mass-discrepancy indicator, with the variation δ_{lum} that would be expected if the luminous matter traced the mass.

These quantities are calculated for the synthesized rotation curves and as many individual rotation curves as possible. Fitting to the obtained data allows for

expressing the mass of dark matter inside R_{opt} and $2R_{opt}$ as a function of the luminosity and rotational speed at R_{opt}. The implications of this can be summarized as follows:

- The fraction of DM increases with the radius.
- The fraction of DM increases, at any normalized radius R/R_{opt}, with decreasing galaxy luminosity.
- The DM is much less concentrated than the LM.

As the distribution of Dark Matter and thus the DM/LM fraction can now be expressed as a function of luminosity and rotational velocity, a formula for a universal rotation curve can be formulated:

$$V_{URC}\left(\frac{R}{R_{opt}}\right) = V\left(R_{opt}\right)\cdot \left[\left(0.72+0.44\log\frac{L}{L_*}\right)\frac{1.97\,x^{1.22}}{\left(x^2+0.78^2\right)^{1.43}} + 1.6\cdot e^{-0.4(L/L_*)}\frac{x^2}{x^2+1.5^2\left(\frac{L}{L_*}\right)^{0.4}}\right]^{1/2} \tag{4}$$

This allows the derivation of galaxy luminosity and therefore measuring the cosmic distance with a typical uncertainty of 0.3 magnitudes by measuring the rotation curve.

3.2 Navarro, Frenk and White 1996&1997

Another approach was done by Navarro, Frenk and White. They used the ever increasing computational power to do N-body simulations, investigating the formation of dark matter halos. This was done for 8 different cosmological models. 5 were Einstein-de Sitter models, two open universe power-law spectra and the ΛCDM model. These models describe the time development of the universe since the Big Bang using Λ ,the cosmological constant, Ω, the density parameter, and n, the scalar spectra index, and thus provide the rules for the simulations.

As the numerical simulations are scale-free by nature, a way to scale the results is needed to compare them with the real world. For this the parameter of the "nonlinear mass" $M_*(z)$ is used. It is defined by requiring that the variance of the linear overdensity field at redshift $z = 0$, smoothed with a top-hat filter enclosing a mass $M = M_*$, should equal the square of the critical density threshold for spherical collapse by redshift z:

$$\Delta_0^2\left[M_*(z)\right] = \delta_{crit}^2\left(z,\Omega_0,\Lambda\right)$$

For the simulation the halos are first identified in cosmological N-body simulations with lower resolution but larger size. Then the individual halos are

resimulated at higher resolutions. The rough simulations were performed on a 128^3 mesh with 10^6 particles and the individual halos are resimulated with $\tilde{}32^3$ particles in a mesh size depending on the virial radius. For the resimulation results of the rough simulation are used as initial conditions, so that resulting halo is similar in all respects to the rough simulation, exept for a improved numerical resolution.

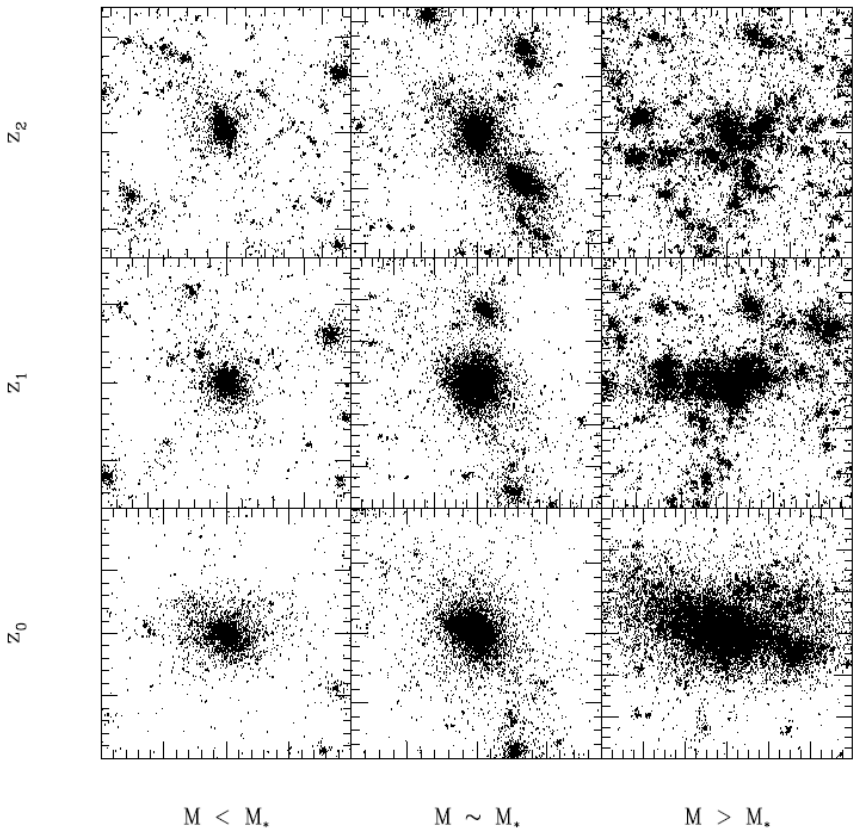

Figure 7: Particle plots illustrating the time evolution of halos of different mass in an $\Omega_o = 1$, $\Lambda = 0$ and $n = -1$ cosmology.

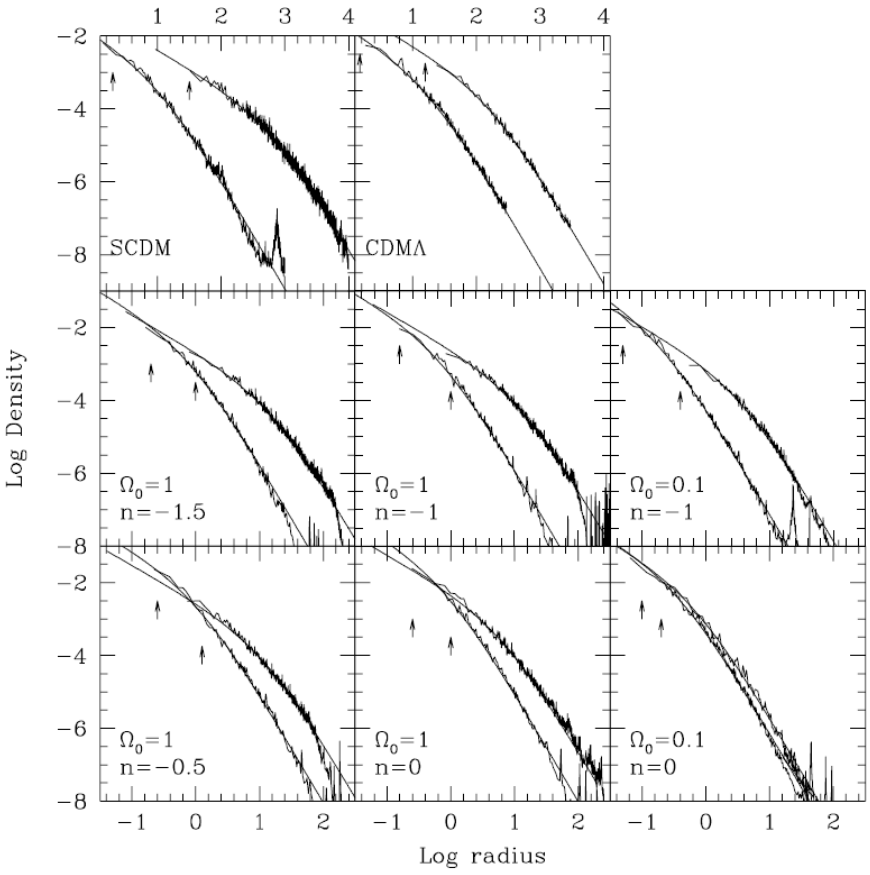

Figure 8: Density profiles of one of the most massive halos and one of the least massive halos in each series for the different cosmological models.

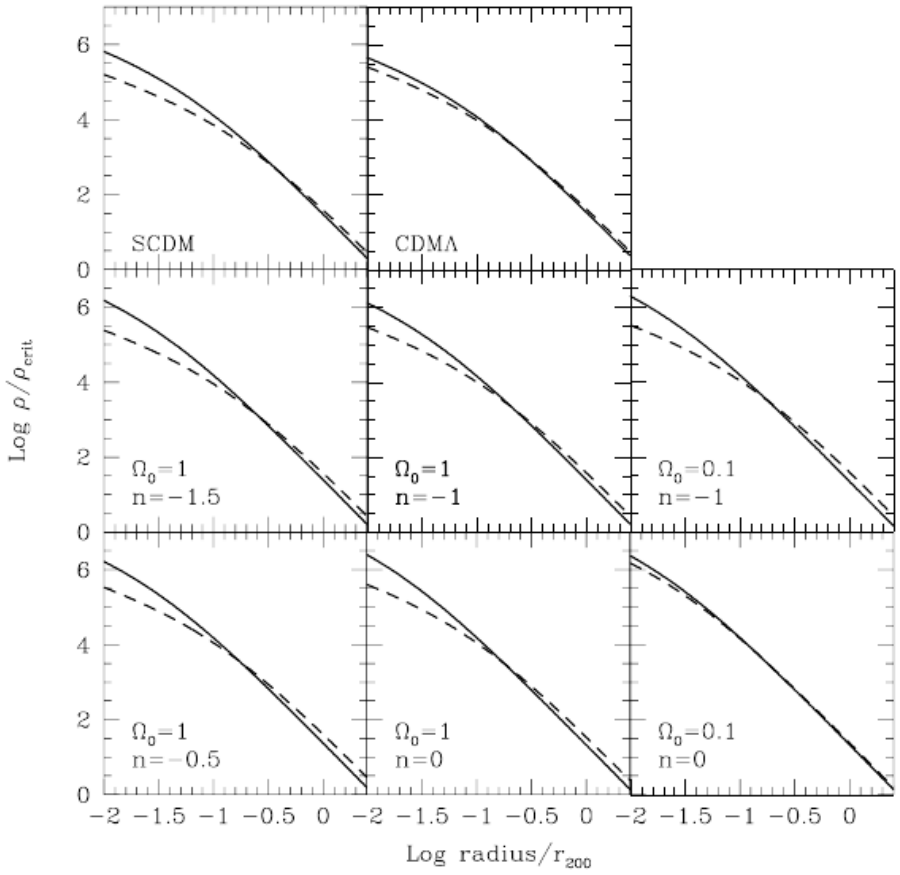

Figure 9: Fits to the density profiles of Fig. 8 scaled to the virial radius r_{200} of each system. The solid lines correspond to low mass halos, the dashed ones to high mass systems.

The simulations have implications similar to the ones Persic, Salluci and Stel made from their analysis of rotation curves:

The lighter halos have higher central DM densities. Additionally it can be seen, that lighter halos assemble faster and that the different cosmological models provide similar results in terms of density profiles. This density profile can be calculated by the following formula and is known today as the NFW profile:

$$\rho\left(r\right) = \frac{3H_o^2}{8\pi G}(1+z_o)^3 \frac{\Omega_0}{\Omega(z_0)} \frac{\delta_c}{cx\left(1+cx\right)^2} \tag{5}$$

$$\text{with: } \delta_c(M,z_0) \sim 3\times 10^3 \Omega\left(z_0\right)\left(\frac{1+z_{coll}}{1+z_0}\right)^3$$

In this $\rho(r)$ is the radius dependent density, H_0 the Hubble constant, G the gravitational constant, z_0 the redshift and z_{coll} the redshift at which the collapse of the halo started.

4 Dark Matter Candidates

After discussing the discovery of Dark Matter through rotation curves and the distribution of it in galactic halos, one might ask, what Dark Matter even is. A sheer endless number of theories have been created, trying to answer this question. The hypothesized particles forming the Dark Matter span a huge range of masses and properties, so only the two extremes for masses will be discussed here.

4.1 Fuzzy Cold Dark Matter[HBG00, Lit18]

One proposed Dark Matter candidate is Fuzzy Cold Dark Matter (FCDM). FCDM consists of extremely low mass particles in the order of $m \sim 10^{-22}$ eV so that their wave properties can manifest on astrophysical scales. For this the de-Broglie wavelength then is

$$\lambda_{db} \approx 2kpc \left(\frac{10^{-22} eV/c^2}{m_a}\right) \left(\frac{10km/s}{v}\right) \tag{6}$$

, with m_a the mass of the axion. This leads to halos which are stabilized by the uncertainty principle of quantum mechanics, just like a hydrogen atom. By this property the formation of initial small-scale structure in DM halos is suppressed. Additionally, because the occupation numbers in the halo become large, the dynamics of the halo can be described similar to the dynamics of a condensate. One issue of this theory is, that due to the very low mass of the particles, a large amount of them is needed, so that a very efficient production mechanism is needed, which can only be non-thermally.

4.2 Primordial Black Holes[KSFM17, KS12, Byr18, Kue18]

Another Dark Matter candidate are primordial Black Holes (PBH). These black holes are assumed to be produced non astronomically, which means that they are not produced by the collapse of a dying star. According to this the masses of primordial black holes are assumed to be much lower than two times the Chandrasekhar limit (2.756×10^{30}kg). This means that for the production of these Black Holes another mechanism must exist. One theory expressed by [Byr18, KSFM17, Kue18] is that the PBH formed during an early stage of the universe. The cosmological density is given by

$$\rho_C = 10^6 \left(\frac{t}{s}\right)^{-2} \frac{g}{cm^3} \tag{7}$$

and the lighter the black holes are, the higher the density required for their production is. A PBH with the mass of only $10^{15}g$ can only be produced spontaneously at $t = 10^{-23}s$ after the Big Bang while a Black Hole the mass of the sun, could still be produced at $t = 10^{-6}s$. This spontaneous production mechanic is easy but probably not efficient enough for the production of large amounts of primordial Black Holes. Instead a production due to cosmic string loops, bubble collisions, pressure reduction or large density perturbations during the QCD phase transition at $t = 10^{-5}s$ [BdS06] appears more likely. The produced black holes are expected to have masses between $10^{20}g$ and $10^{27}g$. Assuming a mass of $10^{20}g$ for all primordial black holes some properties of them can be estimated: The size of such a PBH is around $10^{-8}cm$ and about 10^{25} of them are needed to form the halo of the Milky Way, with an average distance between each PBH of about 10 AU.

5 Conclusion

The observations of rotation curves showed that almost all galaxies have rotation curves with similar properties, with the movement of the luminous matter not following the expected Keplarian motion. This behavior strongly indicates that halos of Dark Matter must exist around galaxies which determines the movement of the luminous matter and thus the rotation curves. The properties of this halo can be estimated using the universal rotation curve of galaxies and N-body simulations, so that a density profile of the halo can be calculated using the NFW profile.

Even though the profile and the effects of dark matter appear somewhat understood the properties of Dark Matter itself remain unclear. Many theories, like PBH and FCDM were developed to explain the nature of the particles DM consists of, but due to the fact, that dark matter remains unobservable directly, no clear favorite can be made out.

References

[BdS06] D. Boyanovsky, H. J. de Vega, and D. J. Schwarz. Phase Transitions in the Early and Present Universe. *Annual Review of Nuclear and Particle Science*, 56:441–500, November 2006.

[Byr18] C. Byrnes. Primordial black hole formation during the QCD phase transition. Kosmologietag 2018, 2018. https://www2.physik.uni-bielefeld.de/fileadmin/user_upload/workshops/RandomProductMatrices/Byrnes.pdf.

[HBG00] W. Hu, R. Barkana, and A. Gruzinov. Fuzzy Cold Dark Matter: The Wave Properties of Ultralight Particles. *Physical Review Letters*, 85:1158–1161, August 2000.

[KS12] K. Kashiyama and N. Seto. Enhanced exploration for primordial black holes using pulsar timing arrays. *MNRAS*, 426:1369–1373, October 2012.

[KSFM17] F. Kuhnel, G. D. Starkman, K. Freese, and A. Matas. Primordial Black-Hole and Macroscopic Dark-Matter Constraints with LISA. *ArXiv e-prints*, May 2017.

[Kue18] F. Kuehnel. New Constraints on Primordial Black Holes as Dark Matter. Kosmologietag 2018, 2018. https://www2.physik.uni-bielefeld.de/fileadmin/user_upload/workshops/RandomProductMatrices/Kuehnel.pdf.

[Lit18] C. Littek. Fuzzy Dark Matter in Kinetic Field Theory. Kosmologietag 2018, 2018. https://www2.physik.uni-bielefeld.de/fileadmin/user_upload/theory_e6/Images/Persons/Littek.pdf.

[NFW96] J. F. Navarro, C. S. Frenk, and S. D. M. White. The Structure of Cold Dark Matter Halos. *The Astrophysical Journal*, 462:563, May 1996.

[NFW97] Julio F Navarro, Carlos S Frenk, and Simon DM White. A universal density profile from hierarchical clustering. *The Astrophysical Journal*, 490(2):493, 1997.

[PSS96] M. Persic, P. Salucci, and F. Stel. The universal rotation curve of spiral galaxies - I. The dark matter connection. *MNRAS*, 281:27–47, July 1996.

[RF70] V. C. Rubin and W. K. Ford, Jr. Rotation of the Andromeda Nebula from a Spectroscopic Survey of Emission Regions. *ApJ*, 159:379, February 1970.

[RFT80] V. C. Rubin, W. K. Ford, Jr., and N. Thonnard. Rotational properties of 21 SC galaxies with a large range of luminosities and radii, from NGC 4605 /R = 4kpc/ to UGC 2885 /R = 122 kpc/. *ApJ*, 238:471–487, June 1980.